Design, solid-phase synthesis and evaluation of enterobactin analogs for iron delivery into the human pathogen Campylobacter jejuni

Citation: Zamora, Cristina Y. et al. "Design, solid-phase synthesis and evaluation of enterobactin analogs for iron delivery into the human pathogen Campylobacter jejuni." Bioorganic & medicinal chemistry, vol. 26, no. 19, 2018, pp. 5314-5321 © 2018 The Author(s)

As Published: 10.1016/J.BMC.2018.04.030

Publisher: Elsevier BV

Persistent URL: https://hdl.handle.net/1721.1/126160

Version: Author's final manuscript: final author's manuscript post peer review, without publisher's formatting or copy editing

HHS Public Access

Author manuscript

Bioorg Med Chem. Author manuscript; available in PMC 2019 October 15.

Published in final edited form as:

Bioorg Med Chem. 2018 October 15; 26(19): 5314–5321. doi:10.1016/j.bmc.2018.04.030.

Design, solid-phase synthesis and evaluation of enterobactin analogs for iron delivery into the human pathogen *Campylobacter jejuni*

Cristina Y. Zamora[a], **Amaël G. E. Madec**[a], **Wilma Neumann**[b], **Elizabeth M. Nolan**[b], and **Barbara Imperiali**[a,b,*]

[a]Department of Biology, Massachusetts Institute of Technology, 77 Massachusetts Avenue, Cambridge, MA 02139, USA

[b]Department of Chemistry, Massachusetts Institute of Technology, 77 Massachusetts Avenue, Cambridge, MA 02139, USA

Abstract

The human enteropathogen *Campylobacter jejuni*, like many bacteria, employs siderophores such as enterobactin for cellular uptake of ferric iron. This transport process has been shown to be essential for virulence and presents an attractive opportunity for further study of the permissiveness of this pathway to small-molecule intervention and as inspiration for the development of synthetic carriers that may effectively transport cargo into Gram-negative bacteria. In this work, we have developed a facile and robust microscale assay to measure growth recovery of *C. jejuni* NCTC 11168 in liquid culture as a result of ferric iron uptake. In parallel, we have established the solid-phase synthesis of catecholamide compounds modeled on enterobactin fragments. Applying these methodological developments, we show that small synthetic iron chelators of minimal dimensions provide ferric iron to *C. jejuni* with equal or greater efficiency than enterobactin.

Graphical abstract

*Corresponding author: Tel.: +1 617 452 1838; fax: +1 617-258-6174; imper@mit.edu (B. Imperiali).

A. Supplementary Data

Supplementary data and spectra can be found in the online version.

Author Contributions

CYZ and BI designed the study with input from EMN and WN; AM developed and applied the SPS and characterized **1** and **2**, WN prepared and characterized **DHB- Ser**; CYZ developed and carried out the microbiological assays, with support from WN and EMN; CYZ, AM and BI wrote the manuscript and all authors analyzed the data and contributed to manuscript preparation.

Conflict of Interest Statement

The Authors declare no competing interests.

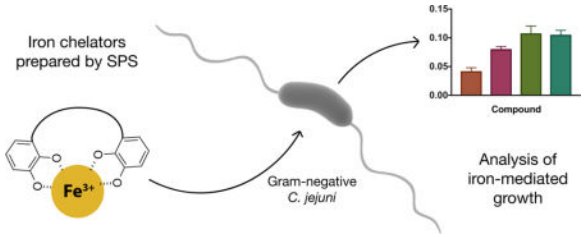

Keywords

Campylobacter jejuni NCTC 11168; Gram-negative pathogens; Iron acquisition; Siderophore; Enterobactin; CfrA; CeuBCDE; Solid-phase synthesis

1. Introduction

The escalation of antibiotic resistance in Gram-negative bacteria is a major human health crisis.[1,2] A particular challenge in *both* the study and treatment of Gram-negative bacterial infections is the complex cell wall structure, which presents a formidable barrier to the uptake of small molecules as biological probes and potential therapeutic agents.[3] Therefore, methods for delivery of small molecules into these organisms represent areas of significant interest. Inspiration for the development of such methods can be found in better understanding of the nutritional requirements of pathogens in human hosts. For example, Gram-negative pathogens *Escherichia coli* and *Pseudomonas aeruginosa* both make use of siderophore-mediated iron uptake pathways. Siderophores are Fe(III)-chelating secondary metabolites that bacteria biosynthesize and secrete during periods of iron limitation to acquire the essential nutrient from the environment.[4] Bacteria that acquire Fe(III) in this way also express specialized siderophore recognition and transport machinery to capture the extracellular Fe(III)-siderophore complexes and deliver them into cells.[5] Recently, siderophore derivatives have been conjugated to various antibiotic cargos,[6–9] including derivatives of enterobactin (**Ent**) (Fig. 1) for delivery *via* enterobactin transport pathways of *P. aeruginosa*[10] and pathogenic *E. coli*.[11,12] These studies highlight the potential for successfully harnessing essential nutrient uptake pathways to deliver small molecules into recalcitrant Gram-negative bacteria.

Study of Gram-negative human enteropathogen *Campylobacter jejuni* NCTC 11168, a leading cause of acute bacterial gastroenteritis, has also revealed paradigms of Fe(III) acquisition,[13,14] as iron is tightly regulated in the intestine of the human hosts but is essential for *C. jejuni* growth.[15] As much as 10^{-7} M iron is required for bacterial survival, yet the poor aqueous solubility at physiological pH and the presence of Fe(III)-binding proteins such as lactoferrin and transferrin maintain free *in vivo* concentrations as low as 10^{-24} M.[16] Interestingly, *C. jejuni* is not known to biosynthesize siderophores, but has evolved several iron uptake pathways[17,18] that take advantage of xenosiderophores, such as **Ent** produced by the commensal microbiotic flora, and Fe(III)-binding proteins in the human gut.[19,20] **Ent** binds Fe(III) with extremely high affinity ($K_a = 10^{49}$ M^{-1})[21] and in *C. jejuni* NCTC 11168 the Fe(III)-**Ent** complex is recognized and transported by a dedicated **Ent** uptake system. The enterobactin iron acquisition pathway comprises six proteins (Fig.

2), which are expressed under low-iron conditions.[13] The outer membrane ligand-gated transporter CfrA binds and transports Fe(III)-**Ent** to the periplasm, where periplasmic-binding protein CeuE, a 36 kD lipoprotein unique amongst Gram-negative bacteria,[22] delivers it to the inner membrane transporter CeuBCD for delivery into the cytosol. Unlike other strains of *C. jejuni*, NCTC 11168 expresses only one outer-membrane transporter (CfrA), as outer-membrane transporter CfrB is encoded as a pseudogene and is not expressed in this strain. Importantly, the Fe(III)- **Ent** acquisition pathway in the *C. jejuni* strains studied has no redundancy[19] and is essential for virulence, evidenced by loss of CfrA abolishing bacterial growth and gut colonization in chickens.[13]

Taken together, these recent findings inspired us to characterize the substrate permissiveness of the Fe(III)-**Ent** uptake pathway in *C. jejuni* towards smaller, synthetically- tractable and readily-functionalizable **Ent** analogs. The choice of lower-denticity compounds was based on recent findings from Raines et al.[23,24] Specifically, structural analysis of CeuE with the **Ent** mimic 4-LICAM (*N,N′*-(butane-1,4-diyl)bis(2,3-dihydroxybenzamide) revealed a 1:1 CeuE:Fe(III)-(4-LICAM) binding mode, suggesting that the CeuBCDE system transports this simplified fragment in complex with Fe(III). Subsequent crystallographic and thermodynamic analyses also revealed that CeuE shows a 100-fold improvement in binding to the tetradentate **Ent** hydrolysis product **(DHB-Ser)$_2$** (Fig. 1), over native **Ent**.[14] Crystallography also showed similar binding modes with the even smaller bidentate catecholamide (2,3-dihydroxybenzoyl)-*L*-serine (**DHB-Ser**), and further efforts revealed significant ligand promiscuity of CeuE.[25] The recent discovery of a periplasmic trilactone esterase Cee (Fig. 2), capable of hydrolyzing **Ent** to **(DHB-Ser)$_2$** and **DHB-Ser** fragments,[26] further supports the view that the **Ent** pathway of the opportunistic pathogen *C. jejuni* accepts and, possibly prefers, smaller **Ent** hydrolysis products.

Herein we report the synthesis and iron-acquisition properties of **Ent** hydrolysis product mimics **1** and **2** (Fig. 1.) Compounds **1** and **2** were prepared by applying a solid-phase synthesis (SPS) approach, which offers practical advantages over solution phase synthesis for this class of compounds and lends itself to facile diversification. Overall, the studies reveal that **1** and **2** facilitate Fe(III)-uptake in *C. jejuni* NCTC 11168, which could prove advantageous and suggests future opportunities for the application of SPS in the synthesis of conjugated analogs that exploit the Fe(III)-acquisition pathway for delivery of probes and bioactive agents into this, and possibly other, Gram-negative pathogens.

2. Results and Discussion

2.1 Design and synthesis of Ent analogs

Inspired by the work of the Stintzi group, which demonstrated that *C. jejuni* is able to utilize a diversity of iron chelators for the uptake of this nutrient,[13] we developed a solid-phase synthesis of minimal **Ent** analogs **1** and **2**, shown in Figure 1. Compound **1** resembles **DHB-Ser**, the minimal **Ent** analog subfragment with Fe(III)-binding properties, and **2** is an analog of **(DHB-Ser)$_2$** wherein the central ester is replaced by an amide to provide enhanced hydrolytic stability. The serine hydroxyl is replaced by an amine as a potential conjugation handle and its positive charge may promote localization to anionic cell surfaces. To our

knowledge, this is the first example of the use of solid-phase elaboration of Ent fragment analogs.

The synthesis begins from N-α-Fmoc-N-β-Alloc-L-2,3-diaminopropionic acid (Fmoc-Dap(Alloc)-OH) **3**, which was immobilized on 2-chlorotrityl polystyrene supported resin (Scheme 1.) The Fmoc-protecting group was removed by treatment with a 4-methylpiperidine solution in DMF, followed by coupling of dibenzylated catechol **5** to the newly-deprotected amine. Once conjugated, N-Alloc group removal was carried out with tetrakis- (triphenylphosphine)palladium ($Pd(PPh_3)_4$ and phenyl silane ($PhSiH_3$), giving **6**. Cleavage of **6** from the resin and Pd/C-catalyzed hydrogenolysis afforded final compound **1** after a brief C_{18} SepPak filtration. Towards biscatechol **2**, a second equivalent of Fmoc-Dap(Alloc)-OH was installed via HBTU-mediated coupling, followed by carbamate reinstallation with allyl chloroformate (Alloc-Cl) to address partial deprotection, giving compound **7**. In the final immobilized step, catechol **5** was conjugated to **7** after N-α-Fmoc removal to yield compound **8**. Cleavage from the resin and subsequent hydrogenolysis gave biscatechol **2**, which was purified by RP-HPLC and obtained in modest yields.

The Fe(III) chelation properties of compounds **1** and **2** were analyzed by UV-Vis spectroscopy (Fig. S6). Both complexes exhibited characteristic catecholate absorption maxima from 285-345 nm. Fe(III)-catecholates, such as ferric **(DHB-Ser)$_2$**, are characterized by broad ligand-to-metal charge transfer (LMCT) bands above 400 nm.[27] We also observed the appearance of a LMCT band (λ_{max} = 450 nm) when compounds **1** and **2** were titrated with $FeCl_3$ in increasing equivalences. These spectral features confirmed formation of Fe(III)-bound species, and based on these results we chose ligand:Fe(III) ratios of 3:1 and 3:2, respectively, for subsequent biological assays with compounds **1** and **2**.

In addition to **1** and **2** prepared by SPS, **Ent**, *D*-enterobactin (**D-Ent**), and **DHB-Ser**, which have been reported to be utilized by *C. jejuni*, were synthesized as described previously.[28,29] With all these compounds in hand, we compared the ability of catecholamides **1** and **2** and **Ent**-type siderophores to mediate transport of Fe(III) into *C. jejuni*.

2.2 Biological evaluation

2.2.1 Microscale assay development—The Fe(III)-**Ent** uptake pathway in *C. jejuni* (Fig. 2) has previously been characterized by growth recovery experiments performed on cultures immobilized in agar. Iron-chelating additives, such as deferrioxamine mesylate, have typically been used to reduce “available” iron concentrations in agar by chelating ferric iron, disallowing its use by the bacterium.[13] Compounds are then placed on this iron-depleted agar in paper disks and any iron transport resulting from their action results in a zone of growth promotion or growth recovery.[13,26] This method cannot distinguish growth inhibition from low growth and does not provide quantitative information on substrate specificity. To address these issues, our goal was to identify low-iron *liquid* growth conditions that consistently supported an attenuated bacterial growth, from which a microscale assay of growth recovery in the presence of additives could be developed. Low-iron conditions would also ensure expression of all necessary Fe(III) transport components shown in Figure 1.

We first characterized growth of *C. jejuni* NCTC 11168 in various iron-depleted media. We chose to modify liquid culture conditions previously utilized for iron-mediated growth recovery in other Gram-negative species, including *E. coli*.[7,11] These conditions included 50% Mueller-Hinton (MH) broth in water containing varying concentrations of 2,2′-bipyridine (BP) to establish iron-deficient conditions, with growth in 50% MH without BP (containing 4.4-5.2 μM iron by ICP-MS) serving as a higher iron growth condition. Control samples were grown in 50% MH broth with the antibiotic ciprofloxacin (Cipro) at the minimal inhibitory concentration (MIC) for *C. jejuni*.[30]

The iron-deficient conditions provided by addition of BP gave undesired binary results with *C. jejuni* grown in microscale cultures, showing no decrease in bacterial growth at low concentrations or inhibiting culture growth to a degree equal to that of Cipro at higher concentrations (Fig. 3A). This trend held also for macroscale cultures over a range of BP concentrations (Fig. S1). Additionally, we found bacterial growth in the iron-deficient conditions could vary significantly between MH broth from different manufacturers or lot batches (data not shown). We therefore evaluated alternative growth conditions and found a chemically defined medium, the minimal essential medium alpha modification (MEM-α), to be the most reproducible for iron-mediated growth measurements at the microscale. MEM-α, containing 0.2 μM iron by ICP-MS analysis, was able to sustain *C. jejuni* cultures and produce a distinct but attenuated amount of bacterial growth relative to MH broth both at microscales (Fig. 3A) and macroscales (Fig. S1). The use of MEM-α also reduced the previously observed sample variability, thereby increasing the robustness of the assay.

Previous studies of enterobactin uptake in *C. jejuni* using **Ent** isolated from microbial sources and siderophore analogs[20] did not investigate the difference in activity between apo- and Fe(III)-bound forms of the chelator. With homogeneous **Ent** obtained *via* chemical synthesis, we were positioned to quantify differential iron recovery provided by apo- and Fe(III)-**Ent**. As shown in Figure 3B, we found that Fe(III)-**Ent** is required to achieve dose-dependent growth recovery down to 0.1 μM in the presented microscale conditions. The growth recovery of cultures observed in 1 μM Fe(III)-**Ent** was equal to that in 9 μM $FeCl_3$, the theoretical highest concentration of soluble ferric iron available at any Fe(III)-**Ent** concentration tested. In stark contrast, administration of apo-**Ent** inhibits growth in the microscale assay (Fig. 3B) and in larger culture volumes (Fig. S2). This inhibition occurs at concentrations of apo-**Ent** that are in 5-fold or higher excess of the concentration of free Fe(III) in the media.

Together, the studies with Fe(III)-**Ent** indicate that the new growth recovery assay provides a robust measure of siderophore-mediated iron transport into *C. jejuni* in microscale liquid cultures. Next, we moved forward to characterize synthetic compounds **1** and **2** in this assay.

2.2.2 C. jejuni growth recovery with Fe(III)-Ent and synthetic iron chelators 1 and 2—To quantify growth recovery, Fe(III) complexes of **1** and **2** were titrated into bacterial cultures in a 96-well plate and growth was measured at 24 h as described above. To ensure stringent iron-depleted conditions, starter cultures of *C. jejuni* were now carried out in iron-poor MEM-α, instead of iron-rich MH, before use in the assay. Growth recovery by

Fe(III)-**Ent** was also measured under these stringent conditions, with Cipro and $FeCl_3$ serving as negative and positive growth controls, respectively.

As shown in Figure 4, all three compounds exhibited dose-dependent iron-mediated growth recovery. Fe(III)-**1** and Fe(III)-**2** recovered growth to an equal degree to Fe(III)-**Ent** at 1 and 10 μM, with apo forms of **1** and **2** having negligible effect on the growth of *C. jejuni* over the same time course (Fig. S3). These results suggest that iron was transported as the ferric chelates of **1** and **2.** Notably, the Fe(III) complex of **1** afforded recovered growth to the same level as Fe(III)-**2** at all concentrations assayed. Although we do not expect a significant amount of free Fe(III) being added along with Fe(III)-**Ent** and the Fe(III)-bound analogs, control assays were carried out in the same concentrations with $FeCl_3$ alone. These cultures (Fig. S4) showed a different pattern of growth recovery from that mediated by Fe(III)-bound compounds. Importantly, Fe(III)-complexed to **1** or **2** at 1 μM induced a greater degree of growth recovery than a bolus (10 μM) of free $FeCl_3$ alone (Fig. 4), suggesting that **1** and **2** participate in iron uptake into the bacterial cytosol.

Overall, the data show that catecholamide derivatives **1** and **2** recover growth in *C. jejuni* NCTC 11168 with comparable efficiency, demonstrating that synthetic fragment **1** is a minimal determinant for iron transport into this organism. Significantly, these derivatives recover growth as well Fe(III)-**Ent**.

2.2.2 Application of microscale assay to the quantification of C. jejuni growth recovery in the presence of known siderophores—We further characterized iron-mediated growth recovery in *C. jejuni* by monitoring growth in the presence of Fe(III)-**DHB-Ser**. This complex may facilitate Fe(III) transport *via* the enterobactin pathway either when recognized directly by CfrA or, when generated in the periplasm by esterase Cee acting on Fe(III)-**Ent** (Fig. 2). In addition, we also monitored growth recovery in the presence of the enantiomeric Fe(III)-**D-Ent**, which is unable to promote growth recovery in *E. coli* as Fes, the cytosolic enterobactin esterase of *E. coli*, cannot hydrolyze this **Ent**-enantiomer to afford iron release.[31] In contrast, Fe(III)-**D-Ent** has been shown to induce growth recovery in *C. jejuni* cultures, but only when the outer membrane receptor CfrA is present,[13] a finding we sought to further characterize by testing in the microscale assay. As above, compounds were titrated into *C. jejuni* cultures in either the apo or ferric forms and the treated bacteria were grown for 24 h in a 96-well plate, followed by OD measurements.

The studies presented in Figure 5 show that Fe(III)-**DHB-Ser** and Fe(III)-**D-Ent** promote growth in *C. jejuni*, with growth at higher concentrations of all compounds reaching optical densities higher than that of $FeCl_3$ alone. Additionally, Fe(III) complexes of **1** and **2** promote growth to a significantly higher degree at concentrations up to 1.0 μM, relative to Fe(III)-**DHB- Ser** (Fig. S5), implying that a single heteroatom substitution (in the case of **1**) also influences growth recovery. Fe(III)-**DHB-Ser** recovered bacterial growth to a significantly lower degree than Fe(III)-**Ent** at all concentrations except the very highest, when all three complexes performed equally well (Fig. 5.) To our knowledge, this is the first report of **Ent**-like function by Fe(III)-**DHB-Ser** in *C. jejuni*. The apo form of **DHB-Ser** did not promote growth, as shown in Figure S3. Significantly, growth recovery in the presence of ferric complexes of **D-Ent** was less efficient at lower concentrations than Fe(III)-**Ent**, suggesting

that the observed growth recovery is a reflection of the siderophore preferences in the enterobactin pathway.

3. Conclusions

In summary, we have presented the synthesis and evaluation of enterobactin analogs for iron delivery into the human pathogen *Campylobacter jejuni* NCTC 11168. The study features a new microscale assay for siderophore-mediated growth recovery in *C. jejuni* that results in growth readouts over a wide dynamic range of ODs capable of distinguishing growth promotion, inhibition, or death. The assay uses 150 μL culture volumes in a 96-well plate format, thereby minimizing total amounts of *C. jejuni* and synthetic compounds needed for a panel of replicate experiments. Furthermore, the assay does not require specialized instrumentation for culture under microaerophilic conditions. We anticipate that this assay will be generally useful for the evaluation of small molecules in this and other strains of *C. jejuni*.

To illustrate the utility of the assay, we demonstrate growth promotion by **Ent** fragment **DHB-Ser**, known to be produced in the periplasm of *C. jejuni* and suspected to bind to components of the inner membrane CeuBCDE transport complex. Additionally, we quantify growth promotion by **D-Ent** and compare it to naturally-occurring **Ent**, revealing inherent substrate preferences of the enterobactin iron-scavenging pathway in *C. jejuni*.

We also describe an efficient SPS approach for the synthesis of the new **Ent** analogs, which can be easily elaborated to produce a wide range of products. The SPS approach is highly practical for this class of molecules as it lends itself to facile optimization and eliminates the need for individual manipulation of conditions for the densely functionalized building blocks. SPS also enables facile target diversification; compounds **1** and **2** are hydrolytically stable and include a primary amine as a chemical handle for functionalization prior to resin deprotection. Furthermore, in the future, the SPS approach can be readily applied to the assembly of targets with alternative commercially-available building blocks. For example, amino acids that feature side-chain azide or alkyne functionality for copper-catalyzed azide/alkyne (CuAAC) cycloaddition while the compounds are still immobilized in the resin could readily be implemented.

By applying the microscale assay and the SPS approach in concert, we have demonstrated that the new synthetic Fe(III)-complexed catecholamides **1** and **2** promote growth at a comparable level to Fe(III)-**Ent**. The Fe(III)-binding properties of these complexes merits further characterization given their growth promotion abilities. The key findings of this study provide a strong foundation for future applications that enlist derivatives of **1** and **2** as conjugation agents that may enable delivery of cargoes including chemical probes as well as antivirulence and antibiotic agents into *C. jejuni*.

4. Experimental procedures

4.1 General information

All standard chemicals and reagents were purchased from Sigma-Aldrich and VWR unless otherwise noted. Following is a list of the sources of other key reagents and expendable materials used in these studies: Polymer-bound 2-chlorotrityl resin, 100-200 Mesh, 1% DVB, 1.4 mmol/g (Novabiochem, 855017); Fmoc-Dap(Alloc)-OH (Bachem (B-2385.0005); 50 mL Torvic solid phase plastic reaction vessels (Torvic); C18 SepPak cartridges (Waters, WAT 023501); BL Mueller-Hinton broth (BD and Co., Cat. No. 211443); ciprofloxacin hydrochloride monohydrate (TCI America, Inc., Cat. No. C2227); ferric chloride (Fisher Scientific, Cat. No. 188-500); MEM-α (Life Technologies, Cat. No. 41061-029); M9 culture media, 5X minimal salts (BD and Co., Cat. No. 248510); Trimethoprim (Chem Impex, Cat. No. 01634); Breathe Easier plate sealing films (Diversified Biotech, Cat. No. BERM-2000); Costar sterile 96-well plates (Corning Incorp., Cat. No. 3595); Oxoid AGS plastic pouches (Invitro Diagnostics, Cat. No., AG0020C); sealing clips for plastic pouches (Invitro Diagnostics, Cat. No. AN0005C); microaerophilic gas mixture for *C. jejuni* growth (85% N_2, 10% CO_2, 5% O_2) (AirGas); culture tubes for macroscale bacterial cultures (17 × 100 mm) (VWR, Cat. No. 60818-689).

4.2 General procedures

Characterization of synthetic intermediates **6-8**, was carried out by cleavage of a sample of the resin, followed by analytical reverse-phase LC-MS using an Agilent Series 1100 HPLC equipped with a YMC AQ12S03-1003WT C18 column and a Finnigan LCQ Deca electrospray ionization mass spectrometer, using a gradient of 5−95% in 20 min of acetonitrile in water with 0.1% TFA. The solid-phase reactor was shaken using an IKA VXR basic vibrax. Isolated compounds **1** and **2** were fully characterized by ^{1}H and ^{13}C NMR and HRMS. ^{1}H and ^{13}C NMR spectra were recorded on a Bruker 400 MHz NMR spectrometer. Chemical shifts (δ) are reported in ppm relative to the residual proton in deuterated DMSO ($(CD_3)_2SO$) at 2.50 ppm for ^{1}H and 39.52 ppm for ^{13}C. HPLC purification of **2** was performed using a Waters 1525 binary HPLC mounted with a 00G-4252-PO-AX (LUNA Co.) preparative column, using a 1% to 23% gradient of MeCN:H_2O with 0.1% TFA.

High-resolution MS spectra of compounds **1** and **2** were collected using direct analysis in real time (DART) ionization on a Bruker Daltonics APEXIV 4.7 T Fourier transform ion cyclotron resonance mass spectrometer (FT-ICR-MS). RP-HPLC purification of **Ent**, **D-Ent**, and **DHB-Ser** was performed on an Agilent 1200 series system with a solvent system, A: 0.1% trifluoroacetic acid (TFA) in Milli-Q water (18.2 mΩ·cm), B: 0.1% TFA in HPLC grade CH_3CN. Absorbance was detected at 220 nm and 316 nm (catecholate absorption) with a multi- wavelength detector. Analytical RP-HPLC was performed using a Clipeus column (C18, 5-μm pore size, 4.6 mm ID × 250 mm; Higgins Analytical) operated at a flow rate of 1 mL min^{-1} and a gradient 0–100% B in A over 30 min. Semi-preparative RP-HPLC was performed using a Zorbax column (C18, 5-μm pore size, 9.4 mm ID × 250 mm; Agilent) operated at a flow rate of 4 mL min^{-1} and a gradient as stated for the respective compounds.

Growth of bacteria on agar plates or in liquid cultures was carried out in a MaxQ6000 incubator shaker (ThermoFisher Scientific); UV-Vis spectroscopy of compounds and optical density measurements of macroscale bacterial cultures were performed in disposable 1.5 mL cuvettes on a Nanodrop 2000C (ThermoFisher Scientific); optical density measurements of microscale assays were performed on a SynergyH1 microtiter plate reader (Biotek). ICP-MS analysis was carried out on an Agilent 7900 ICP mass spectrometer.

4.3. Synthesis of and characterization of compounds

4.3.1 Synthesis of compounds 1 and 2

4.3.1.1 Generalized procedure A for analysis of resin-bound intermediates: In order to cleave an analytical sample of resin-bound intermediate, a sample of resin was transferred from the main reactor to a 1.5-mL Eppendorf containing 1.0 mL of CH_2Cl_2:TIPS:TFA (95:2.5:2.5). The mixture was then shaken for 30 min at room temperature. The solvent was removed under a flow of nitrogen. The resulting residue was dissolved in CH_3CN and the polystyrene beads of the resin were filtered using a syringe filter. The crude mixture was then submitted to LC-MS analysis.

4.3.1.2 Synthesis of 4: The 2-chlorotrityl resin (2.0 g, 2.80 mmol) was charged in a solid-phase reaction reactor. The resin was swelled in anhydrous CH_2Cl_2 by shaking at room temperature for 20 min. The solvent was then removed. In a separate vial, Fmoc-Dap(Alloc)-OH (920 mg, 2.24 mmol) was dissolved in 15 mL of CH_2Cl_2 and DIPEA (1.56 mL, 9.96 mmol) and transferred to the solid-phase synthesis reactor containing the swelled resin and was allowed to react at room temperature for 2 h on the shaker. The resin was subsequently washed three times with 20 mL of DMF and three times with 20 mL of CH_2Cl_2. The resin was then treated with a solution of CH_2Cl_2:DIPEA:MeOH (17:2:1, 20 mL) for 1h at room temperature to cap unreacted 2- chlorotrityl chloride. Following this the resin was filtered and washed three times with 20 mL of DMF and three times with 20 mL of CH_2Cl_2.

4.3.1.3 Synthesis of 6: Compound **5** was synthesized as previously reported.[32] The solid-phase reactor containing **4** was filled with 15 mL of 20% solution of 4-methylpiperidine in DMF. The reactor was shaken for 20 min at room temperature. The resin was subsequently washed three times with 20 mL of DMF and three times with 20 mL of CH_2Cl_2. The same protocol was repeated once. Then 2,3- bis(benzyloxy)benzoic acid (**5**) (1.12 g, 3.36 mmol) and HBTU (1.70 g, 4.48 mmol) were dissolved in 10 mL of DMF. DIPEA (1.56 mL, 9.96 mmol) was slowly added to the reaction mixture containing **5** and HBTU, which was allowed to react 5 min at room temperature before being added to the solid-phase reactor containing **4**. The reaction was carried out for 45 min at room temperature. The resin was subsequently washed three times with 20 mL of DMF and three times with 20 mL of CH_2Cl_2. The reaction progress was followed by LC-MS analysis of a cleaved sample of the resin, following general procedure A. $C_{28}H_{29}N_2O_7$ $[M+H]^+$: 505.19, found: 505.07. Next, Alloc deprotection was carried out under anhydrous conditions. To a scintillation vial equipped with a screw cap septum, $Pd(PPh_3)_4$ (51.7 mg, 0.045 mmol) was added. The vial was purged with N_2, then 10 mL of anhydrous THF was added followed by $PhSiH_3$ (552 μL, 4.48 mmol). The mixture was then transferred to the solid-phase reactor that had been

purged with N_2 to minimize oxidation of the catalyst. The reaction was carried out at room temperature for 20 min. The resin was subsequently washed three times with 20 mL of DMF and three times with 20 mL of CH_2Cl_2. The resin was re-subjected to the reaction following the above procedure to yield **6**. The reaction progress was followed by LC-MS analysis following general procedure A. $C_{24}H_{25}N_2O_5[M+H]^+$: 421.17, found: 421.20.

4.3.1.4 Synthesis of (S)-3-amino-2-(2,3-dihydroxybenzamido)propanoic acid 1: A quantity of resin representing 0.24 mmol (by mass % of the total mass resin) was added to a 20-mL solid-phase reactor. The compound was cleaved off the resin by addition of a solution of 3.0 mL of CH_2Cl_2:TIPS:TFA (95:2.5:2.5), for 1 h at room temperature. The eluate from the solid-phase reactor was collected and concentrated *in vacuo*. The crude residue was transferred to a 10-mL round-bottom flask and dissolved in 2.4 mL of MeOH, then 20% Mw $Pd(OH)_2/C$ (3.4 mg, 0.024 mmol), was added to the reaction. The reaction flask was purge under H_2 for 5 min, then kept under a positive pressure of H_2 with a hydrogen balloon. The reaction progress was followed by LC-MS analysis and was determined to be complete in 30 min. The crude product was filtered through Celite®, concentrated *in vacuo* and then purified on a SepPak C18 light plus cartridge, using a gradient from 95:05 to 75:25 of H_2O/MeCN, yielding the TFA salt of the desired product as a reddish brown amorphous solid, (40 mg, 69%). ^{1}H NMR (400 MHz, DMSO-d_6) δ: 9.23 (1H, d, J = 7.8 Hz, N**H**), 8.23 (3H, s, N$\mathbf{H}_3^+$), 7.44 (1H, d, J = 8.1 Hz, Ar**H**), 6.98 (1H, d, J = 7.8 Hz, Ar**H**), 6.72 (1H, t, J = 7.9 Hz, Ar**H**), 4.76 (1H, dt, J = 8.5, 4.4 Hz, NH- C**H**), 3.41 – 3.20 (m, 2H, C$\mathbf{H}_2$) partially obscured by residual water peak; ^{13}C NMR (101 MHz, DMSO) δ: 170.3 (**C**(O)), 170.1 (**C**(O)), 149.3 (Ar), 146.2 (Ar), 119.3 (Ar), 118.2 (Ar), 118.1 (Ar), 115.1 (Ar), 50.4 (**C**-C(O)-OH), 45.4 (**C**H_2); $C_{10}H_{13}N_2O_5$, MS (ESI): m/z $[M+H]^+$ calculated for 241.0819 Da, found 241.0819 Da.

4.3.1.5 Synthesis of 7: Fmoc-Dap(Alloc)-OH (1.38 g, 3.36 mmol) and HBTU (1.70 g, 4.48 mmol) were dissolved in 10 mL of DMF. To this solution, DIPEA (1.56 mL, 9.96 mmol) was slowly added. The mixture was allowed to react 5 min before being added to the solid-phase reactor containing immobilized **6**. The reaction was carried out for 45 min at room temperature. The resin was subsequently washed three times with 20 mL of DMF and three times with 20 mL of CH_2Cl_2. Allyl chloroformate (2.38 mL, 22.4 mmol) was dissolved in 15 mL of anhydrous CH_2Cl_2, DIPEA (3.9 mL, 22.4 mmol) was subsequently added to the mixture. The solution was transferred onto the resin and stirred for 1 h at room temperature. The resin was subsequently washed three times with 20 mL of DMF and three times with 20 mL of CH_2Cl_2. The reaction progress was followed by LC-MS analysis of a cleaved sample of the resin, following general procedure A. $C_{46}H_{45}N_4O_{10}[M+H]^+$: 813.30, found: 813.13.

4.3.1.6 Synthesis of 8: The solid-phase reactor containing **7** was filled with 15 mL of a 20% solution of 4- methylpiperidine in DMF. The reactor was shaken for 20 min at room temperature. The resin was subsequently washed three times with 20 mL of DMF and three times with 20 mL of CH_2Cl_2. The same protocol was repeated once. Then 2,3-bis(benzyloxy)benzoic acid (**5**) (1.12 g, 3.36 mmol) and HBTU (1.70 g, 4.48 mmol) were dissolved in 10 mL of DMF. DIPEA (1.56 mL, 9.96 mmol) was slowly added to this mixture, which was allowed to react 5 min at room temperature before being added to the

solid-phase reactor containing **7**. The reaction was carried out for 45 min at room temperature. The resin was subsequently washed three times with 20 mL of DMF and three times with 20 mL of CH_2Cl_2. The reaction progress was followed by LC-MS analysis following general procedure A $C_{52}H_{51}N_4O_{11}$ $[M+H]^+$: 907.35, found: 907.13 Da.

4.3.1.7 Synthesis of (S)-3-(((S)-2-carboxy-2-(2,3-dihydroxybenzamido)ethyl)amino)-2-(2,3- dihydroxybenzamido)-3-oxopropan-1-aminium (2): A quantity of resin representing 0.36 mmol (by mass % of the total resin mass) was added to another solid-phase reactor. Alloc deprotection was carried out under anhydrous conditions. To a scintillation vial equipped with a screw cap septum, $Pd(PPh_3)_4$ (6.6 mg, 0.06 mmol) was added. The vial was purged with N_2, then 4 mL of anhydrous THF was added followed by $PhSiH_3$ (71.4 μL, 0.58 mmol). The mixture was transferred to the solid-phase reactor that had been flushed with N_2 to minimize oxidation of the catalyst. The reaction was carried out at room temperature for 20 min. The resin was subsequently washed three times with 20 mL of DMF and three times with 20 mL of CH_2Cl_2. The reaction progress was followed by LC-MS analysis of a cleaved sample of the resin, following general procedure A, $C_{48}H_{47}N_4O_9$ $[M+H]^+$: 823.33, found: 823.27. The compound was cleaved off the resin by addition of 3.0 mL of a solution of CH_2Cl_2:TIPS:TFA (95:2.5:2.5) to the solid-phase reactor which was shaken for 1 h at room temperature. The elution from the solid-phase reactor was collected and concentrated *in vacuo*. The crude was transferred to a 10-mL round-bottom flask and dissolved in 2.4 mL of MeOH, then 20 % Mw $Pd(OH)_2/C$ (5.0 mg, 0.036 mmol) was added to the reaction. The reaction flask was purged with H_2 for 5 min, then kept under a positive pressure of H_2 with a hydrogen balloon. The reaction progress was followed by LC-MS analysis and was determined to be complete in 30 min. The crude product was filtered on Celite®, concentrated and purified by reverse phase HPLC (1 to 23 % MeCN:H_2O with 0.1 % TFA), yielding 15 mg (9%, 0.03 mmol) of the TFA salt of the product as a white fluffy solid. ^1H NMR (400 MHz, DMSO-d_6) δ:13.03 (1H, s, COO**H**), 11.97 (2H, s, C-O**H**), 9.32 (2H, s, C-O**H**), 8.98 (1H, d, *J* = 8.0 Hz, N**H**), 8.92 (1H, d, *J* = 7.5 Hz, N**H**), 8.50 (1H, t, *J* = 5.9 Hz, N**H**), 7.96 (3H, s, N$\mathbf{H}_3^+$), 7.34 (1H, dd, *J* = 8.2, 1.5 Hz, Ar**H**), 7.29 (1H, dd, *J* = 8.2, 1.5 Hz, Ar**H**), 6.96 (2H, app ddd, *J* = 7.7, 6.1, 1.5 Hz, 2 × Ar**H**), 6.72 (2H, app q, *J* = 8.0 Hz, 2 × Ar**H**), 4.77 (1H, td, *J* = 8.5, 4.4 Hz, NH-C**H**-CH_2-NH_3^+), 4.58 (1H, td, *J* = 7.9, 4.8 Hz, NH-C**H**-C(O)OH), 3.76 (1H, dt, *J* = 13.6, 5.5 Hz, C$\mathbf{H}_A$CH_B-NH), 3.11 (1H, dd, *J* = 13.1 Hz, 9.0 Hz, CH_AC$\mathbf{H}_B$-NH), The 2 protons C$\mathbf{H}_A$C$\mathbf{H}_B$-NH_3^+ are obscured by residual H_2O; ^{13}C NMR (101 MHz, DMSO-d_6) δ: 171.5 (C(O)), 170.1 (C(O)), 169.6 (C(O)), 169.1 (C(O)), 149.3 (Ar), 149.2 (Ar), 146.4 (Ar), 146.3 (Ar), 119.3 (Ar), 119.3 (Ar), 118.6 (Ar), 118.4 (Ar), 118.18 (Ar), 118.1 (Ar), 115.7 (Ar), 115.0 (Ar), 52.4 (NH-**C**H), 51.0 (NH-**C**H), 40.2 (CH_2). Note: one carbon is hidden beneath the solvent peak. $C_{20}H_{23}N_4O_9$, MS (ESI): m/z $[M+H]^+$ calculated for 463.1460 Da, found 463.1460 Da.

4.3.1.8 Generalized procedure for characterization of Fe(III) chelation by UV-Vis spectroscopic titration: Compound **1** (9.5 mg, 0.0345 mmol) was vortexed until dissolved in H_2O (1.5 mL). In a separate vessel, a 20 mM solution of $FeCl_3$ in 0.3 M HCl was prepared and briefly vortexed to give a bright yellow solution. Into each of 5 eppendorf tubes was dispensed 13.1 μL of **1**, followed by 0-13.5 μL $FeCl_3$ solution (0-0.9 eq.) and mixed, immediately yielding dark blue solutions. All aqueous mixtures, appearing dark

grey-green, were incubated overnight at 4 °C. Volumes were completed to 1 mL in MeOH and immediately transferred to a cuvette for UV-Vis analysis. Final concentrations of Fe(III) chelate in all samples was 300 μM. The UV/Vis absorption spectra of samples were measured from 200-700 nm and compared to cuvettes containing MeOH only. Compound **2** (1.3 mg, 2.8 μmol) was dissolved in H_2O (490 μL) and each of 5 eppendorf tubes received 51.7 μL of **2**. All 5 samples were mixed with 0-0.9 eq of $FeCl_3$ and analyzed for ferric iron chelation following the same procedure described above.

***4.3.2 Preparation of* Ent, D-Ent, and DHB-Ser—Ent** and **D-Ent** were synthesized as previously reported.[29]

Enzymatic Preparation of DHB-Ser: The *E. coli* enterobactin esterase IroD was overexpressed in *E. coli* BL21(DE3) as a N-terminal His_6-fusion protein and purified by Ni-NTA affinity chromatography as previously reported.[28] A 5-mL solution containing **Ent** (500 μM) was prepared in 75 mM Tris-HCl buffer, pH 8.0 and divided into five 1-mL aliquots. IroD (1 μM) was added to each 1-mL aliquot of Ent and the reactions were incubated at room temperature for 1.5 h. Each reaction was quenched by the addition of 6% TFA in Milli-Q water (100 μL per aliquot) and concentrated by lyophilization. The resulting concentrate was dissolved in 2:1 H_2O/dioxane, and purified by semi-preparative HPLC (0–20% B over 10 min; elution at 9.5 min). The retention time corresponded to a standard sample and no further analysis was performed.

4.3.3 Generation of ferric species of compounds 1, 2, Ent, DHB-Ser, and D-Ent—Catechol **1** in water (3 eq., clear, colorless solution) was added to a 20 mM $FeCl_3$ solution separately prepared in 0.3 M HCl (1 eq., light yellow solution) and vortexed to produce Fe(III)-**1** (dark grey-green solution) after 30 min at room temperature. Similarly, biscatechol **2** (3 eq., clear colorless solution) was added to 20 mM $FeCl_3$ (2 eq.) and vortexed to produce Fe(III)-**2** as a clear, indigo solution. Ferric complexes were generated one day prior to growth recovery assays and stored at −20 °C until use. Fe(III)-complexed native siderophores were generated as above immediately before use: **Ent** (1 eq. to 0.9 eq Fe(III)), **D-Ent** (1 eq. to 0.9 eq Fe(III)), and **DHB- Ser** (3 eq. to 1 eq Fe(III)). All apo solutions were clear and colorless, Fe(III)-**Ent** and Fe(III)-**D- Ent** formed clear indigo solutions, and Fe(III)-**DHB-Ser** gave a dark blue-green solution.

4.4 Microscale assay development and application

4.4.1 Growth conditions for C. jejuni starter cultures—Samples from glycerol stocks of *C. jejuni* (NCTC 11168) were streaked onto MH agar plates containing selection antibiotic trimethoprim (50 μg/mL). Plates were placed inside a plastic pouch (along with an atmospheric CO_2 indicator) and purged with a microaerophilic gas mixture (85% N_2, 10% CO_2, 5% O_2) multiple times until the correct concentration of CO_2 was reached. Sealed pouches were then incubated at 37 °C for 24 h, after which colonies were taken up in 3 mL of MH broth or MEM-α media containing necessary selection antibiotics. A 3-mL aliquot of MH broth or MEM-α media in a culture tube was inoculated with 15 μL of the above bacterial suspension and incubated in microaerophilic pouches for 24 h 37 °C, oriented at 45 degrees and shaking at 190 rpm, to produce the final starter culture. In our hands, starter

cultures of wild type *C. jejuni* (11168) grown in this manner routinely reach an optical density of 1.5 after 24 h in MH or 0.5 in MEM-α. Once grown, cultures are used immediately in growth assays described below.

4.4.2 Evaluation of C. jejuni growth in various media conditions—To evaluate the growth of *C. jejuni* in various media, cultures were inoculated and grown at macro- and microscale. For macroscale experiments, 3-mL aliquots of MH broth, 50% MH broth in water, M9 medium or MEM-α medium were dispensed into culture tubes and trimethoprim added. Ciprofloxacin at 0.5 mg/mL (MIC for *C. jejuni*) was added as an additional control, while $FeCl_3$ was added as a positive control for iron-promoted growth. A 1-mL aliquot was taken from a *C. jejuni* starter culture, washed once with PBS by centrifugation at 15,000 $\times g$ for 1 min, and re-suspended in 1 mL of PBS. Cultures were inoculated with washed bacteria to an initial OD_{600} of 0.015, placed in microaerophilic pouches and grown at 37 °C for 24 h, as described for starter culture growth. In our hands, an OD_{600} of 0.015 corresponded to 1×10^7 cfu/mL. OD_{600} were measured in a cuvette at the end of the experiment, and the background absorbance of the corresponding broth or media subtracted to give the adjusted optical density. For microscale experiments, 100 μL of broth of interest containing selection antibiotics and other compounds was dispensed into 6 wells in a 96-well plate. To each well, 50 μL of the same media composition containing washed bacteria was added to give a final optical density of 0.015 in the well. Once all wells were inoculated (final volume 150 μL), a Breathe Easier film was utilized to cover the plate and it was placed in a plastic pouch, purged with the microaerophilic gas mixture, and incubated at 37 °C for 24 h with shaking at 190 rpm. Each 96-well plate was immediately read at 600 nm to measure optical density and no visible pellets formed during bacterial growth.

4.4.3 Microscale growth recovery assay of C. jejuni in the presence of Ent and Ent analogs—The ability of apo- and Fe(III)-**Ent** analogs to promote growth recovery was assayed in a 96-well plate. Briefly, solutions of MEM-α were made in 1.7-mL microcentrifuge tubes containing selection antibiotics and various concentrations of apo- or Fe(III)-siderophores. MEM-α containing ciprofloxacin served as a negative control for growth, while solutions of MH broth instead of MEM-α were made to elicit growth recovery and be used as a positive control. Once made, solutions were inoculated with *C. jejuni* grown in either MH (iron rich) or MEM-α (iron poor) starter cultures as previously described to a starting OD_{600} of 0.015. Then, 150 μL of each solution was plated into a 96-well plate in duplicate or quadruplicate and the plate covered with a Breathe Easier film. Plates were placed in microaerophillic pouches, grown, and the OD_{600} read as described above. Three independent experiments were performed to give n = 6 or more per compound.

Supplementary Material

Refer to Web version on PubMed Central for supplementary material.

Acknowledgments

We thank Elizabeth Ward for technical assistance and our research groups for helpful discussions. We also thank Dr. Phoom Chairatana of the Nolan lab for providing samples of **Ent** and **D-Ent**. Financial support from the NIH (R01-GM097241 to B.I.) and (1R21AI126465 and 1R01AI114625 to E.M.N.) is gratefully acknowledged. W.N.

acknowledges the German National Academy of Sciences Leopoldina for a postdoctoral fellowship (LPDS 2015-08). We are also grateful to MIT CEHS Bioanalytical Core (NIH grant P30-ES002109) and the MIT Chemistry Department DCIF for ICP-MS, NMR and HR-MS analyses.

Abbreviations

BP	2,2′-bipyridine
CH_2Cl_2	dichloromethane
Cipro	ciprofloxacin
DIPEA	*N,N*-diisopropylethylamine
DMF	dimethylformamide
DMSO	dimethylsulfoxide
ICP-MS	inductively coupled plasma mass spectrometry
MeCN	acetonitrile MEM-α: minimal essential medium alpha modification
MH	Mueller-Hinton
MIC	minimal inhibitory concentration
PBP	periplasmic-binding protein
PBS	phosphate-buffered saline
HBTU	(2-(1*H*-benzotriazol-1-yl)-1,1,3,3-tetramethyluronium hexafluorophosphate)
SPS	solid-phase synthesis
TFA	trifluoroacetic acid
THF	tetrahydrofuran
TIPS	triisopropylsilane

References

1. Global priority list of antibiotic-resistent bacteria to guide research, discovery, and development of new antibiotics. World Health Organization (WHO); Geneva: 2017.
2. Brown ED, Wright GD. Nature. 2016; 529:336–343. [PubMed: 26791724]
3. Tommasi R, Brown DG, Walkup GK, Manchester JI, Miller AA. Nat Rev Drug Discov. 2015; 14:529–542. [PubMed: 26139286]
4. Hider RC, Kong X. Nat Prod Rep. 2010; 27:637–657. [PubMed: 20376388]
5. Miethke M, Marahiel MA. Microbiol Mol Biol R. 2007; 71:413–451.
6. Ji C, Juárez-Hernández RE, Miller MJ. Future Med Chem. 2012; 4:297–313. [PubMed: 22393938]
7. Zheng T, Bullock JL, Nolan EM. J Am Chem Soc. 2012; 134:18388–18400. [PubMed: 23098193]
8. Page MGP. Ann NY Acad Sci. 2013; 1277:115–126. [PubMed: 23346861]
9. Tillotson GS. Infect Dis. 2016; 9:45–52.
10. Ji C, Miller PA, Miller MJ. J Am Chem Soc. 2012; 134:9898–9901. [PubMed: 22656303]

11. Zheng T, Nolan EM. J Am Chem Soc. 2014; 136:9677–9691. [PubMed: 24927110]
12. Chairatana P, Zheng T, Nolan EM. Chem Sci. 2015; 6:4458–4471. [PubMed: 28717471]
13. Palyada K, Threadgill D, Stintzi A. J Bacteriol. 2004; 186:4714–4729. [PubMed: 15231804]
14. Raines DJ, Moroz OV, Blagova EV, Turkenburg JP, Wilson KS, Duhme-Klair AK. P Natl Acad Sci USA. 2016; 113:5850–5855.
15. Hofreuter D. Front Cell Infect Microbiol. 2014; 4:1586–1605.
16. Raymond KN, Dertz EA, Kim SS. P Natl Acad Sci USA. 2003; 100:3584–3588.
17. Stahl M, Butcher J, Stintzi A. Front Cell Infec Microbiol. 2012; 2:5–15. [PubMed: 22919597]
18. Miller CE, Williams PH, Ketley JM. Microbiol. 2009; 155:3157–3165.
19. Xu F, Zeng X, Haigh RD, Ketley JM, Lin J. J Bacteriol. 2010; 192:4425–4435. [PubMed: 20585060]
20. Naikare H, Butcher J, Flint A, Xu J, Raymond KN, Stintzi A. Metallomics. 2013; 5:988–996. [PubMed: 23702883]
21. Loomis LD, Raymond KN. Inorg Chem. 1991; 30:906–911.
22. Park SF, Richardson PT. J Bacteriol. 1995; 177:2259–2264. [PubMed: 7730251]
23. Raines DJ, Moroz OV, Wilson KS, Duhme-Klair AK. Angew Chem Int Ed Engl. 2013; 52:4595–4598. [PubMed: 23512642]
24. Müller A, Wilkinson AJ, Wilson KS, Duhme-Klair AK. Angew Chem Int Ed. 2006; 45:5132–5136.
25. Wilde EJ, Hughes A, Blagova EV, Moroz OV, Thomas RP, Turkenburg JP, Raines DJ, Duhme-Klair AK, Wilson KS. Sci Rep. 2017; 7:45941–45955. [PubMed: 28383577]
26. Zeng X, Mo Y, Xu F, Lin J. Mol Microbiol. 2013; 87:594–608. [PubMed: 23278903]
27. Scarrow RC, Ecker DJ, Ng C, Liu S, Raymond KN. Inorg Chem. 1991; 30:900–906.
28. Lin H, Fischbach MA, Liu DR, Walsh CT. J Am Chem Soc. 2005; 127:11075–11084. [PubMed: 16076215]
29. Ramirez RJA, Karamanukyan L, Ortiz S, Gutierrez CG. Tetrahedron Lett. 1997; 38:749–752.
30. Oh E, Jeon B. Front Microbiol. 2015; 6:52–59. [PubMed: 25762984]
31. Abergel RJ, Zawadzka AM, Hoette TM, Raymond KN. J Am Chem Soc. 2009; 131:12682–12692. [PubMed: 19673474]
32. Leydier A, Lin Y, Arrachart G, Turgis R, Lecerclé D, Favre-Reguillon A, Taran F, Lemaire M, Pellet-Rostaing S. Tetrahedron. 2012; 68:1163–1170.

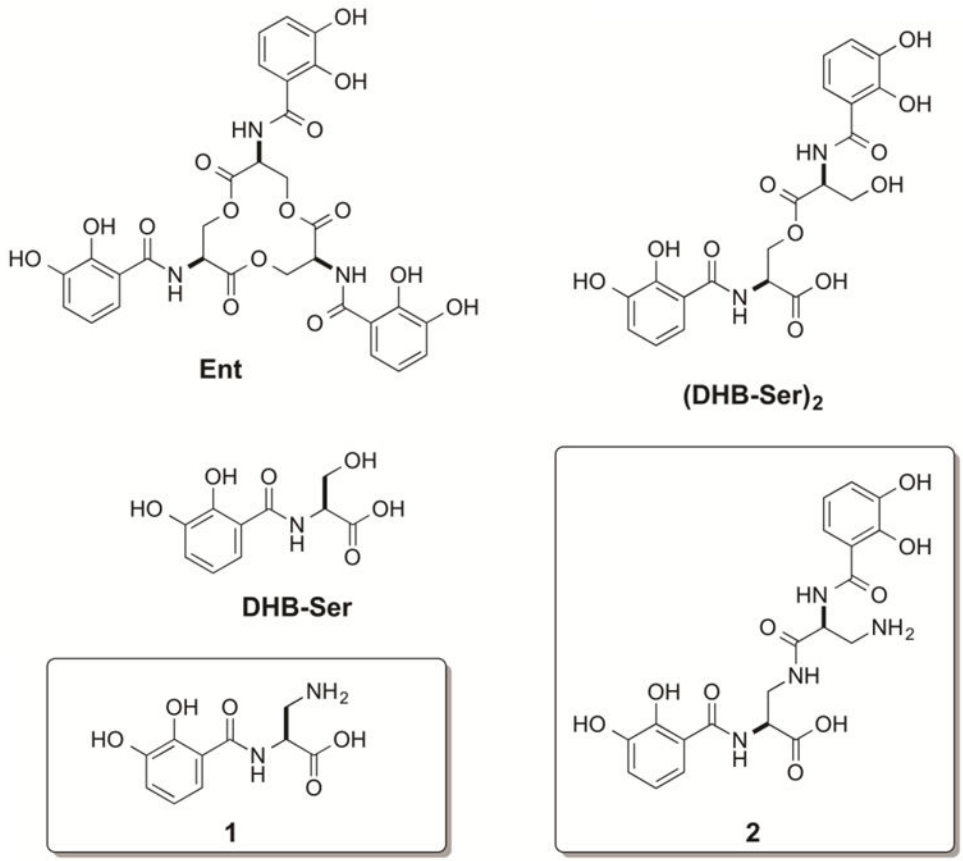

Figure 1.
Structures of key compounds relevant to this study.

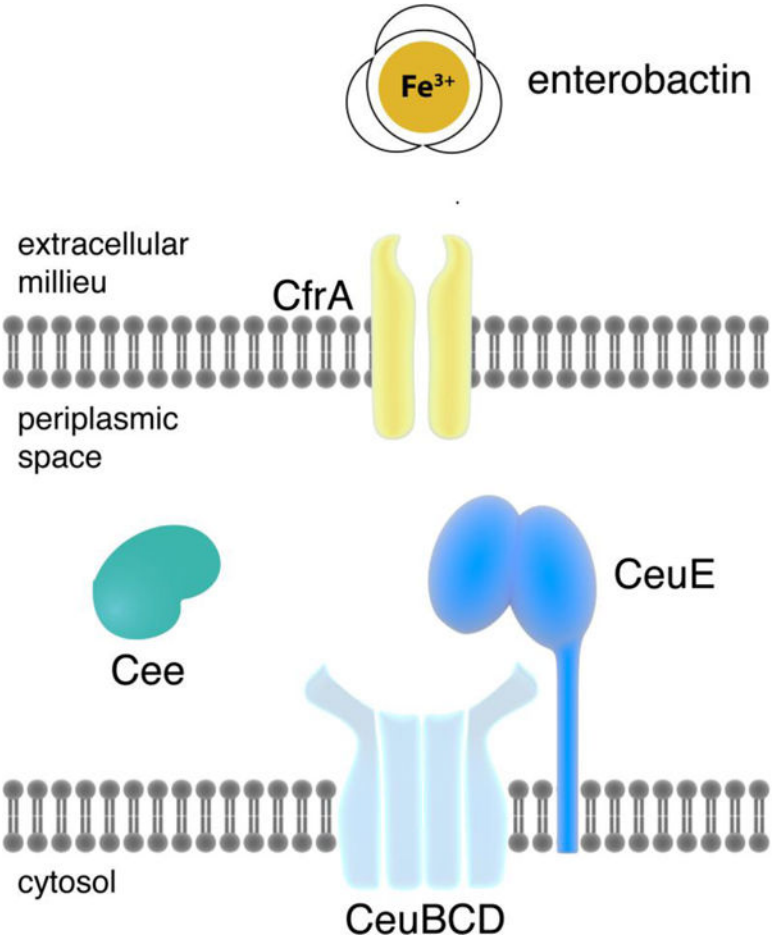

Figure 2.

Illustration of the Fe(III)-**Ent** acquisition pathway in *C. jejuni* NCTC 11168. Enterobactin (depicted as three crescent moons) is shown chelating ferric iron, shown as an orange circle. Outer membrane ligand-gated transporter CfrA translocates Fe(III)-**Ent** from the extracellular milieu to the periplasmic space. There, Fe(III)-**Ent** may be bound by PBP CeuE for delivery to inner membrane transporter CeuBCD. Alternatively, Fe(III)-**Ent** may be hydrolyzed by trilactone esterase Cee into smaller Fe(III)-chelated fragments, which are then transported to the cytosol by CeuBCD for Fe(III) release.

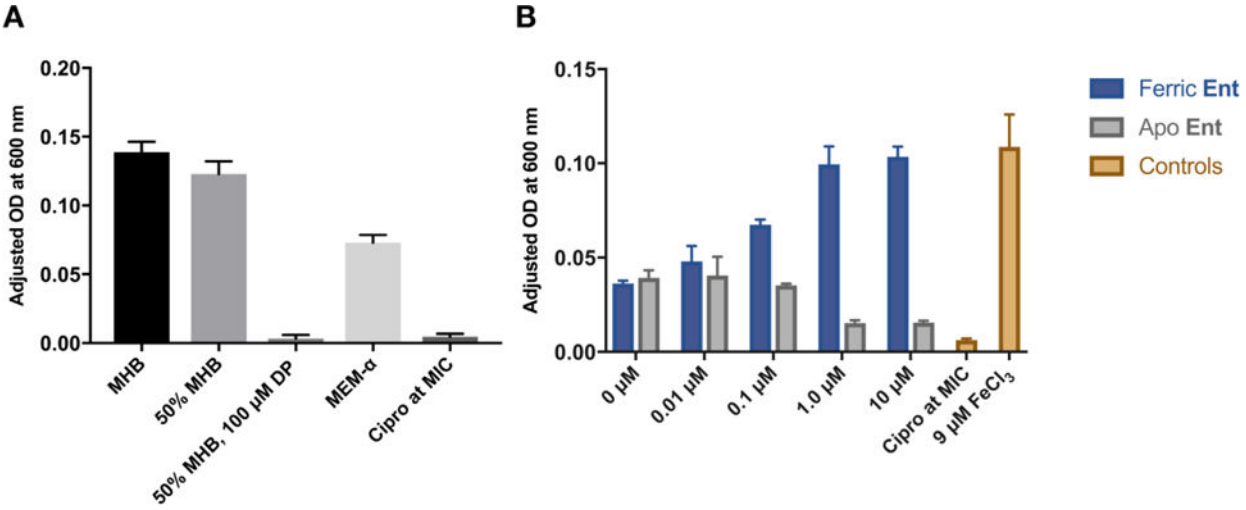

Figure 3.

Growth of *C. jejuni* in conditions of varying iron availability. A) *C. jejuni* were grown in indicated media (150 μL) for 24 h under microaerophilic conditions. B) Titration of Fe(III)-**Ent** initiates dose-dependent growth recovery, while titration of apo-**Ent** into *C. jejuni* cultures results in growth inhibition. Cultures of *C. jejuni* in MEM-α (150 μL) were provided varying amounts of apo or ferric **Ent** in a 96-well plate and grown under microaerophilic conditions for 24 h. Data shown are end-point OD_{600} measurements. Background absorbance of broth or media at 600 nm was subtracted from raw OD_{600} measurements to give the adjusted OD_{600}. Data is representative of multiple independent experiments. (n = 4, mean +/− SDM)

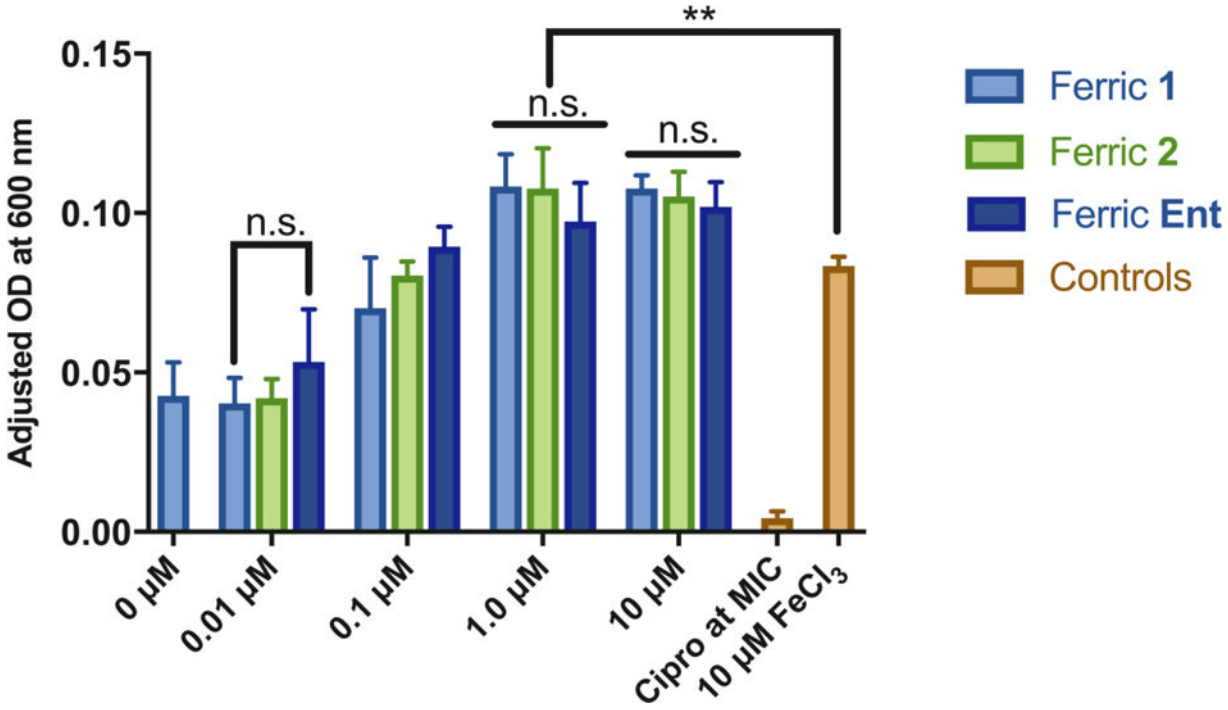

Figure 4.

Synthetic ferric **Ent** analogs **1** and **2** recover iron-mediated growth of *C. jejuni* as well as, or better than, known Fe(III)-**Ent**. Cultures of *C. jejuni* in MEM-α (150 μL) were provided varying amounts of each Fe(III)- chelated compound in a 96-well plate and grown under microaerophilic conditions for 24 h. Data shown are end- point OD_{600} measurements. The background absorbance of the media at 600 nm was subtracted from raw OD_{600} measurements to give the adjusted OD_{600} with no further normalization. Bars represent the mean of three independent experiments, in which each condition was executed in duplicate. Error bars show one SD. ** indicates P<0.005. Statistical analysis performed using unpaired Student's t-test with Welch's correction in GraphPad Prism.

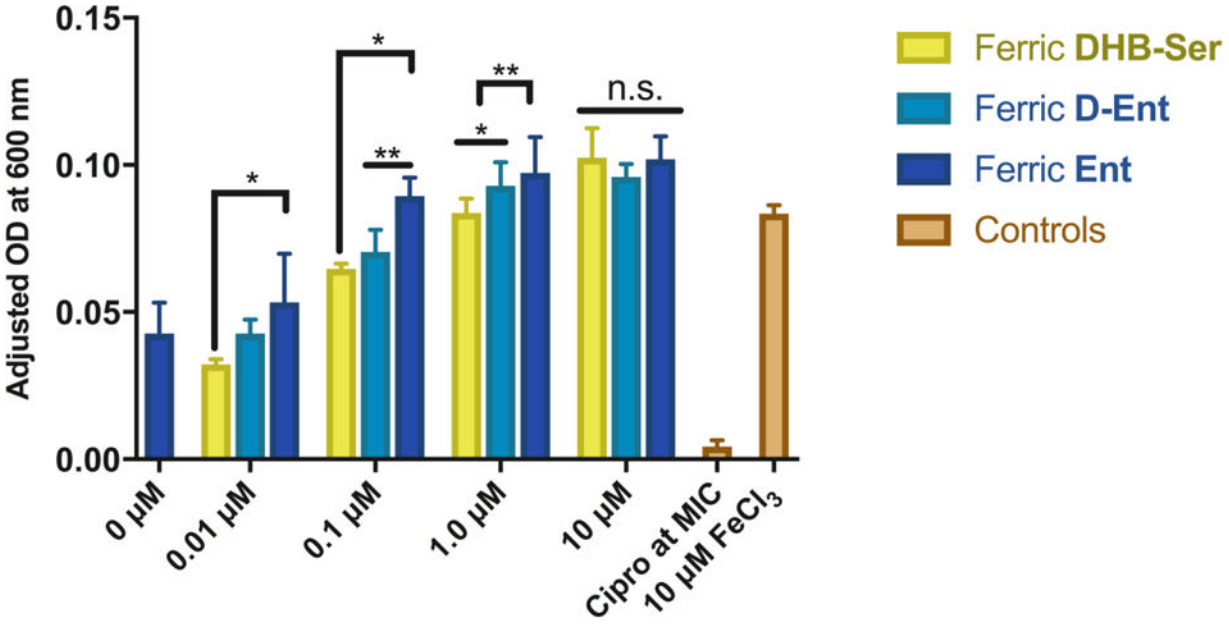

Figure 5.

Fe(III)-**Ent**, Fe(III)-**DHBSer** and Fe(III)-D-**Ent** differentially recover iron-mediated growth of *C. jejuni*. Cultures of *C. jejuni* in MEM-α (150 μL) were provided varying amounts of each ferric compound in a 96-well plate and grown under microaerophilic conditions for 24 h. Data shown are end-point OD_{600} measurements. Bars represent the mean of three independent experiments, in which each condition was executed in duplicate. Background absorbance of media at 600 nm was subtracted from raw OD_{600} measurements to give the adjusted OD_{600} with no further normalization. Error bars show one SD. ** Indicates $P<0.005$ and * indicates $P<0.05$. Statistical analysis performed using unpaired Student's t-test with Welch's correction in GraphPad Prism.

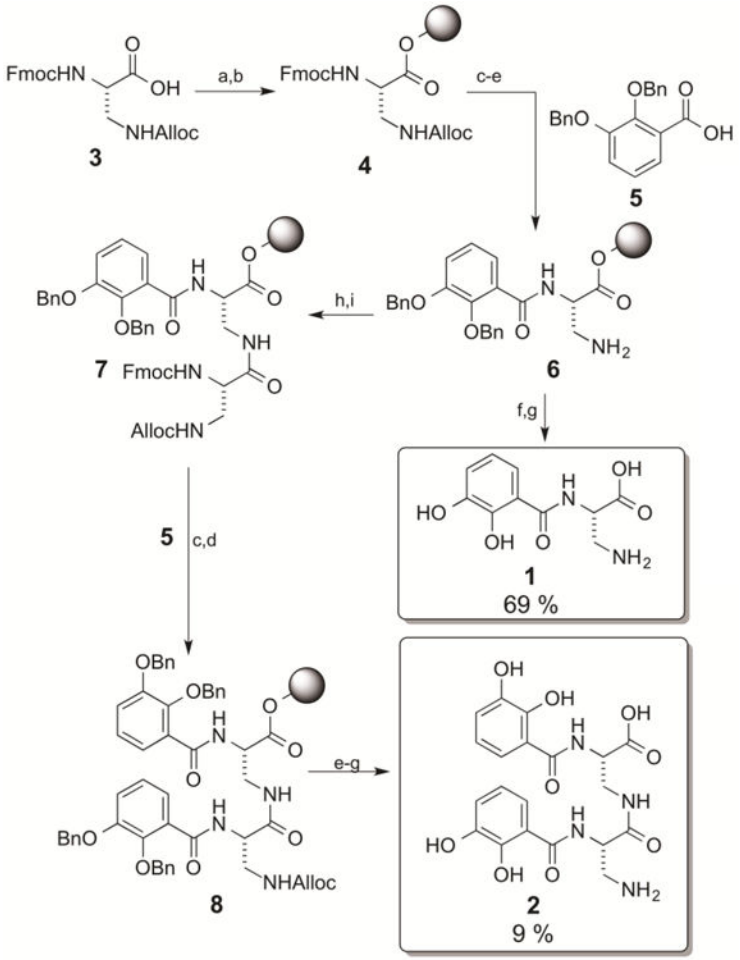

Scheme 1.

a) 2-Chlorotrityl chloride resin, DIPEA, CH_2Cl_2, rt, 1 h; b) CH_2Cl_2, DIPEA, MeOH, rt, 30 min; c) 4-Methyl-piperidine 20% in DMF, 20 min, rt; d) HBTU, **5**, DIPEA, DMF, rt, 45 min; e) (Pd(PPh3)4)., $PhSiH_3$, THF, rt, 20 min; f) CH_2Cl_2, TIPS, TFA; g) $Pd(OH)_2$, H_2, MeOH, rt, 30 min; h) HBTU, Alloc-Dap(Fmoc)-OH, DIPEA, DMF, 45 min; i) Alloc-Cl, DIPEA, CH_2Cl_2, rt, 1 h.